Parametric Analysis of Elastic Impact Models

A. Kiedrzynski, S. Verbiese

Université Libre de Bruxelles, Institut de Mécanique Appliquée, 50 av. D.F. Roosevelt, B-1050 Bruxelles, Belgium

SUMMARY. The simplest structural impact model retaining the inertia and deformability properties of both missile and target is parametrically investigated for different models of loading conditions. The paper discusses the circumstances for which the system can readily be linearized, as well as an upper bound for missile internal forces. Finally, an "equivalent" spring-dashpot massless target, which can be beneficial for models of large nuclear components wrt computer time, is evaluated.

1. INTRODUCTION

In nuclear engineering, one often faces the task of evaluating the various consequences of the impact between a large component (e.g.piping or vessel) in movement, called missile, and another fixed elastic body, generally the civil engineering structure, called target - fig. 1a. The impact may result from a pipe rupture type of accident or an earthquake.

In order to capture basic physical facts about the impact phenomenon, the research effort has concentrated on the smallest building block of a large dynamic model : i.e. a 3-dof linear system consisting of a 1-mass structural target connected to the ground through a spring stiffness, and a 2 mass by spring connected missile striking the target through a 1-spring bumper - fig. 1b. Previous experimental research demonstrated [2] the small influence of material damping on the impact phenomena allowing to discard this entry in the parametric study. Hence the system of fig. 1b. retaining the inertial and elastic nature of both missile and target, is expressed in a nondimensional format using 4 parameters. With the following frequency notations (see fig. 1b)

$$\omega_m^2 = \frac{k_m}{m_2} , \quad \omega_T^2 = \frac{k_T}{m_T} , \quad \omega^2 = \frac{k}{m_1} \qquad (1abc)$$

where ω is the frequency of the reference system (fig.1e) in which the stiffness k is given by

$$\frac{1}{k} = \frac{1}{k_b} + \frac{1}{k_T} , \qquad (1e)$$

the 4 nondimensional parameters choosen are :

$$\gamma_m^2 = \frac{\omega^2}{\omega_m^2} , \quad \gamma_T^2 = \frac{\omega^2}{\omega_T^2} , \quad \mu_2 = \frac{m_2}{m_1} , \quad \mu_T = \frac{m_T}{m_1} . \qquad (2\ abcd)$$

With this choice of parameters, the stiffnesses $k_{m,b,T}$ appear implicitly and are expressed by the following relations :

$$\frac{k}{k_m} = \frac{\gamma_m^2}{\mu_2} , \quad \frac{k}{k_b} = 1 - \frac{\gamma_T^2}{\mu_T} , \quad \frac{k}{k_T} = \frac{\gamma_T^2}{\mu_T} < 1 \qquad (3\ abc)$$

Fig. 1b shows the fundamental model, where the missile is assumed to be free from external constraints and loads during the total impact period. At time $t = 0$, it strikes the target with the initial velocity v_o and is internally unconstrained prior to the first contact with the bumper.

Two other models feature a loaded missile. For the one of fig. 1c, the missile masses m_1 and m_2 are loaded respectively by forces m_1a and m_2a proportional to their inertias and the impact again starts at time $t = 0$. In this case the following additional fifth nondimensional parameter influences the impact phenomenon :

$$q = \frac{a}{\omega v_o} . \qquad (4)$$

For the model of fig. 1d, at time $t = 0$, the mass m_2 of the missile is suddenly loaded by a constant force P; at this moment the gap between the mass m_1 and the bumper is h and the missile is internally unconstrained. Here the additional fifth nondimensional parameter is

$$\lambda = h \frac{k}{P} \qquad (5)$$

where P/k is the displacement of the mass m_1 under the static action of the force P. This model could be used for a rough 1-d representation of an impact generated by a pipe rupture.

The numerical analysis was carried out using modal analysis.

As the equipment designers are primarily interested in the missile integrity, the analysis is focused on the internal missile forces.

Low impact velocities and elastic behaviour of both colliding structures are assumed.

2. DISPLACEMENTS AND INTERNAL FORCES IN THE SYSTEM.

Fig. 2 presents, for the model of fig. 1b, typical plots of the nondimensional displacements $(\omega/v_o)\ X_{1,2,T,}$ and the displacement $(\omega/v_o)X_G$ of the mass centroid of the missile, versus the nondimensional time ωt. Under certain conditions (figs. 2 c and 2 e) successive rebounds of mass m_1 may appear, "microshocks" separated by "microseparations", during the whole "macroshock", consisting itself in the approach and departure of the missile center of gravity and spanning the period between first contact and last separation. These microshocks introduce the sole source of nonlinearity in the study: opening and closing of the gap dictate the splitting of the calculation in contact and separation phases, necessitating each a separate system of modal analysis equations connected by temporal boundary conditions, to obtain a close-form time-history solution of the phenomenon.

The absence of microseparations during impact (fig. 2 abd) allows the use of one same linear 3-dof system for the whole impact period. In the presence of microseparations, the occurrence of but small gap amplitudes suggests the linearization of using the same advantageous 3-dof modal analysis formalism for the whole impact period (gap edges kept "sticking" together): only minor effects on the impact phenomenon and, more importantly, on the force levels, are recorded; if now these gap amplitudes are important, the internal force in the missile reaches a maximum during microseparations, and in this case the above linearization would lead to false conclusions. The authors have shown in ref. [3] that this case is found with the two following circumstances :

1) great values of γ^2_m which means - see (3a) - a very deformable missile, and small or moderate values of μ_2 - fig. 2c.

2) great values (close to unity) of the ratio γ_T/μ_T which means - see (3b) - a very stiff bumper.

In these circumstances however, when the missile is loaded by external forces (models of figs 1cd), the gap amplitudes during micro-separations appear to be reduced if these forces are important, i.e. if, for the case of fig. 2c, the parameter q defined by (4) is important, or if for the case of fig. 2d, the value of the parameter λ defined by (5) is not very high. Indeed, fig. 3b shows the displacements of the same set of parameters as this of fig. 2e but the missile is loaded as on fig. 1c, by forces of magnitude expressed by $q=1$. The gap amplitudes during microseparations are very small and, again, the above linearization can be confidently applied - fig. 3d.

Figs 3c and 3e represent corresponding nondimensional forces.

$$f_{m,b,T} = F_{m,b,T} \quad \frac{\omega}{kv_o} \tag{6}$$

in the missile (m), bumper (b) and target (T); fig. 3e gives the forces for the linearised model. The internal force in the missile (m) is not quite affected by the linearization.

Fig. 4 represents the plots of the displacements and forces for the loading model of fig. 1d. Here, the nondimensional displacements and forces are respectively defined as :

$$\xi_{1,2,T} = X_{1,2,T} \cdot \frac{k}{P} \qquad p_{m,b,T} = \frac{F_{m,b,T}}{P} \tag{7ab}$$

The values of the four fundamental parameters (2 abcd) are identical to these of fig.2e. Figs. 4b and 4c show the displacements and forces for $\lambda = 10$ - see (5).
The linearised calculations are again successfully applied, as presented on figs. 4de.

The missile loaded by forces pointing towards the target, will evidently undergo multiple rebounds as a whole : "macroshocks" alternating with "macroseparations". When comparing fig. 3a with fig. 3b, and fig. 4a with fig. 4b, it appears that the amplification of the loading forces (greater q or smaller λ) leads to :
- amplification of the period of a macroshock
- reduction of the period of a macroseparation
- reduction of the total period of a macroshock + macroseparation.

3. EFFECT OF THE TARGET CHARACTERISTICS ON THE MAXIMUM INTERNAL FORCE IN THE MISSILE.

As the loaded missile undergoes multiple macroshocks with different initial conditions for each of them, the maximum internal force in the missile varies for each macroshock "n"; its nondimensional value for the loading model of fig. 1d, can be expressed as follows :

$$(p_{m,n})_{max} = \sum_{i=1}^{3} p_{m,n}^{(i)} \sin (\Omega_i \tau \quad \theta_n^{(i)}) + 1 \qquad (8)$$

where Ω_i is the angular frequency of the i-th mode, $p_{m,n}^{(i)}$ and $\theta_n^{(i)}$ are respectively the amplitudes and phase angles corresponding to the mode "i" within the macroshock "n" and the time τ is calculated from the beginning of this macroshock. The missile internal force will never exceed

$$\max(p_{m,n})_{max} = \sum_{i=1}^{i} \left| p_{m,1}^{(i)} \right| + 1 \qquad (9)$$

where $p_{m,1}^{(i)}$ corresponds to the first macroshock.

Fig. 5 shows two interesting features of the influence of the target parameters μ_T and γ_T^2/μ_T on this upper bound of the missile internal forces (9) :

a) for small values of μ_T and γ_T^2/μ_T (bumper much more flexible than target) the missile internal force is practically independent of the target characteristics.

b) for γ_T^2/μ_T = const. this force as a function of the target mass ratio μ_T reaches a minimum; indeed, if μ_T is either very small or very high the target exhibits no inertial damping; for moderate values of μ_T, the inertial damping reaches its maximum which influences favourably the reduction of the internal force in the missile. On fig. 5 the dotted lines indicate maximas of p_m drawn from time-history.

4. EQUIVALENT NON INERTIAL TARGET

When large nuclear components are evaluated numerically for earthquakes or pipe ruptures, the civil engineering structures are generally considered only through their equivalent interface properties,i.e. the storing of vibration energy in the impacted civil engineering structural masses is often simulated by using artificial viscous dampers between component and ground nodes - fig. 6.

On the SMiRT-6 conference, the authors have justified their opinion [2], that the real equivalence criterion for the value of the damping ratio η in the equivalent model-fig. 6, is the equality of internal forces.

The diagram of fig. 7 represents the internal force in the missile $(\bar{p}_m)_{max}$ in the equivalent model, as a function of the damping ratio η. The diagrams of fig. 8 represent the equivalent damping ratio η for the missile of fig. 5, as functions of the target characteristics. It is obtained by equating $(\bar{p}_m)_{max} = \max\,(p_m)_{max}$.

For an assumed value of η (say 10%), the conservativity region is located between the two slopes of the curve corresponding to the given value of γ^2_T/μ_T (say .3 - see thick line on the diagram of fig. 8).

5. CONCLUSIONS.

- Each set of nondimensional parameters γ^2_m, γ^2_T, μ_2, μ_T and q or λ gives access through time-history plots of nondimensional displacements and forces, to a wide spectrum of elastic structural impact applications presenting the same basic phenomenological features.
- The occurrence and characteristics of the general rebound (macroshock) and the local

rebounds (microshocks) are depicted for typical cases.

- When interested in the maximum forces in the missile, one may use a straightforward linearization ignoring the microshocks, except for situation with very deformable missiles or very stiff bumpers, in the presence of small to moderate external forces on the missile.
- Macroshock frequency is a function of missile loading.
- The upper bound of the force in the missile in nonsensitive to target characteristics for a wide range of cases, and presents a minimum depending of target characteristics.
- Selecting a simpler "equivalent" (in terms of maximum missile internal force) massless but damped target is possible for certain parametrical circumstances.

6. AKNOWLEDGMENTS.

Authors are glad to express their gratitude to MM. A. LAURENT and Ph. KENNES, students at Brussels University, for their kind help in the numerical computations.

7. REFERENCES.

1) J.C. HENNART, "Study and Measurements of Impact Damping in PWR Reactor Coolant System Seismic and Accident Restraints", SMiRT-5, Berlin, 1979.

2) A. KIEDRZYNSKI, L. COPPENS and S. VERBIESE, "Analysis, Measurement and Modelisation of Impact Damping", SMiRT-6, Paris, 1981.

3) A. KIEDRZYNSKI, L. COPPENS and S. VERBIESE, "Analyse de modèles d'impact entre structures élastiques", Journées Vibrations-chocs, Lyon, 1982.

4) A. LAURENT, "Etude du choc entre structures élastiques", Travail de fin d'études à l'Université de Bruxelles, 1982.

5) P. KENNES, "Etude du choc entre structures élastiques", Travail de fin d'études à l'Université de Bruxelles - to appear.

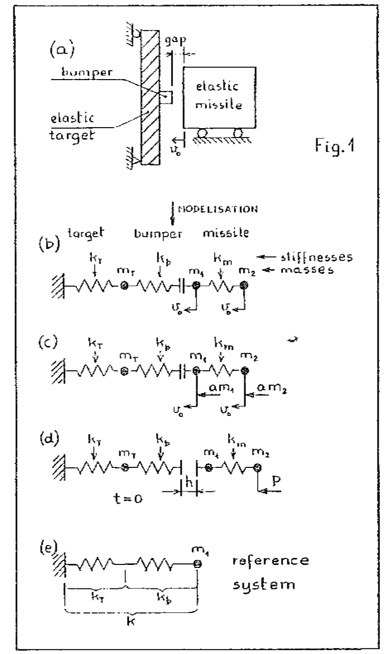

Fig.1

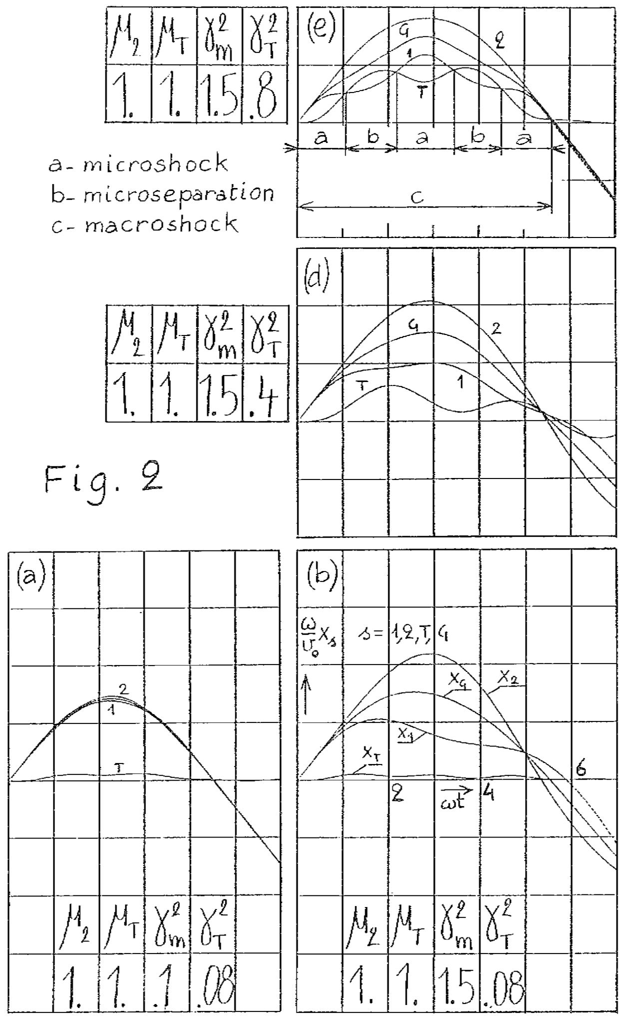
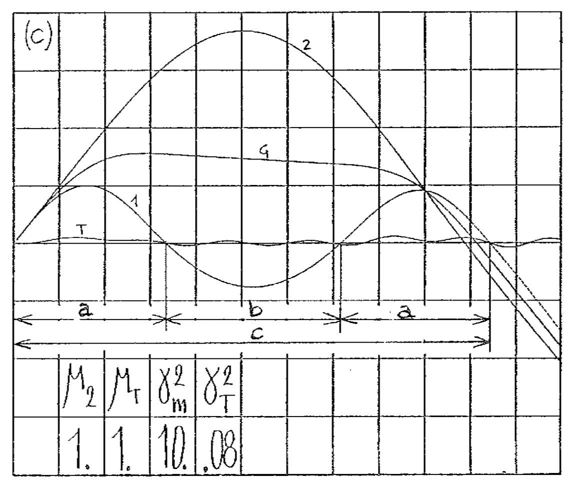

μ_2	μ_T	γ_m^2	γ_T^2
1.	1.	.1	.08

μ_2	μ_T	γ_m^2	γ_T^2
1.	1.	1.5	.08

μ_2	μ_T	γ_m^2	γ_T^2
1.	1.	10.	.08

μ_2	μ_T	γ_m^2	γ_T^2
1.	1.	1.5	.4

μ_2	μ_T	γ_m^2	γ_T^2
1.	1.	1.5	.8

Fig. 2

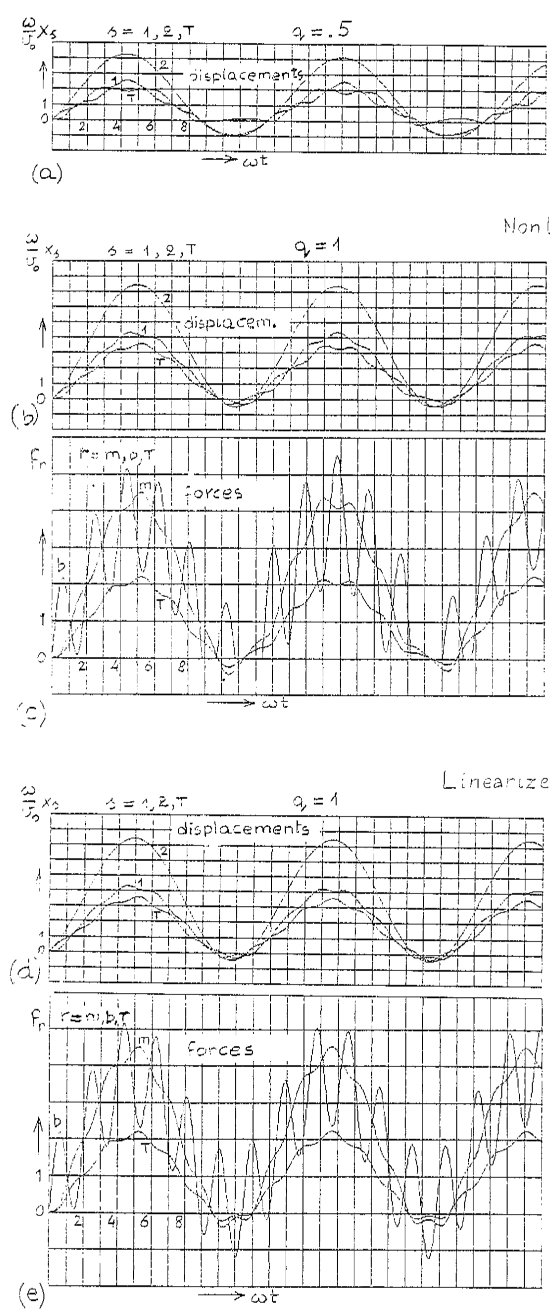

μ_2	μ_T	γ_m^2	γ_T^2
1.	1.	1.5	.5

Fig. 3

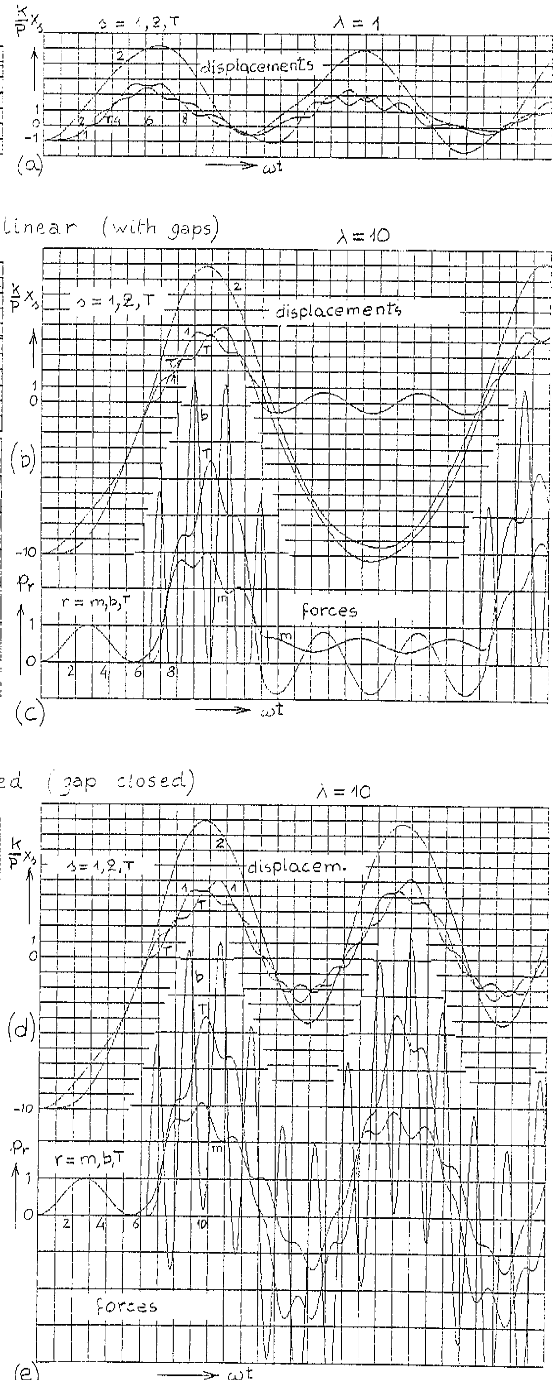

Fig. 4

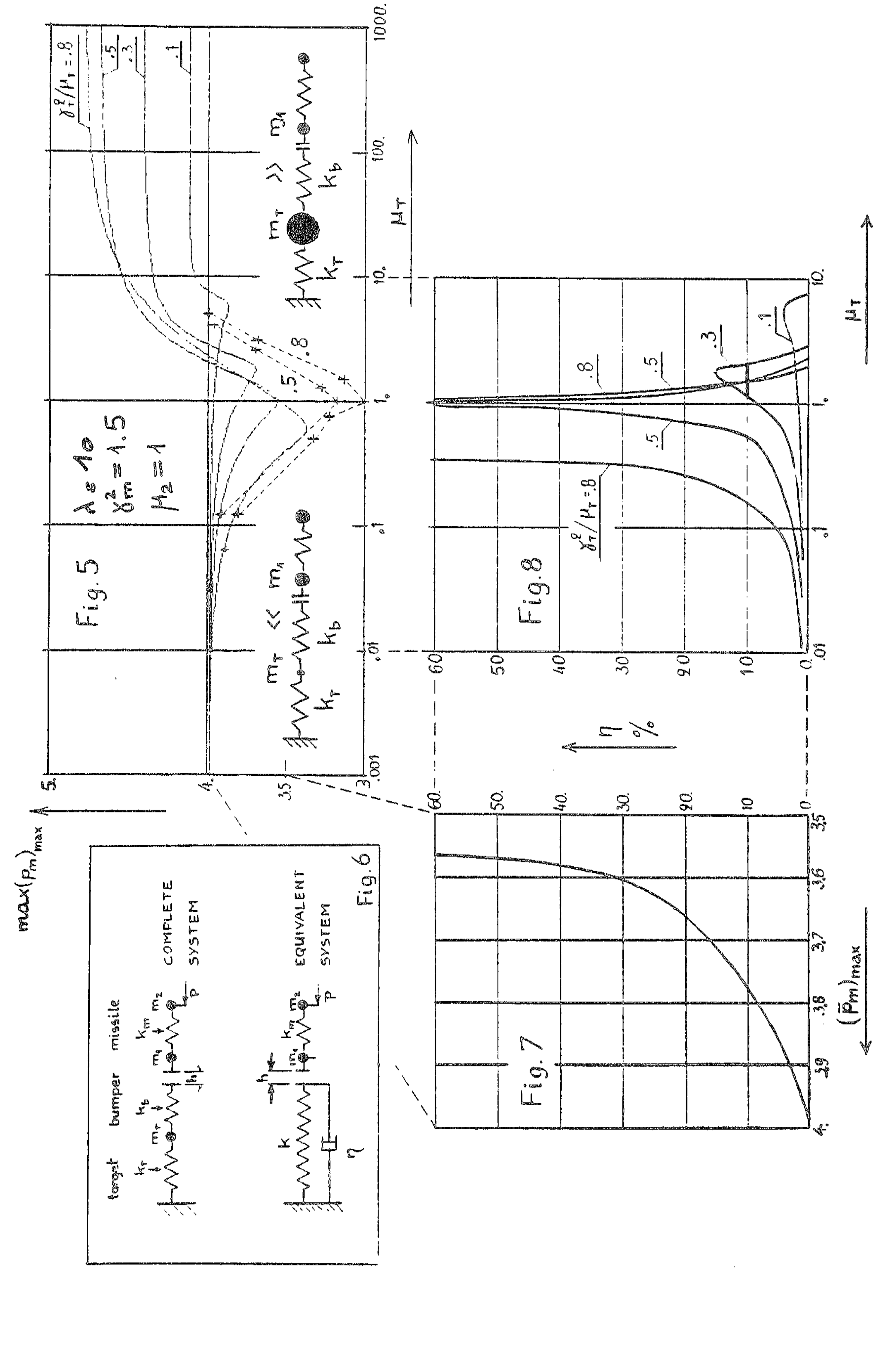
Fig. 5
Fig. 6
Fig. 7
Fig. 8
target
bumper
missile
COMPLETE SYSTEM
EQUIVALENT SYSTEM
λ = 10
γm² = 1.5
μ2 = 1
max(pm)max
η %
(p̄m)max
μT